ORIGINAL RESEARCH

VISTA (PD-1H) Is a Crucial Immune Regulator to Limit Pulmonary Fibrosis

Sang-Hun Kim[1], Taylor S. Adams[1], Qianni Hu[2], Hyeon Jun Shin[1], Ganghee Chae[3], Sang Eun Lee[3], Lokesh Sharma[1], Hyuk-Kwon Kwon[4], Francis Y. Lee[4], Hong-Jai Park[5], Won Jae Huh[6], Edward Manning[1], Naftali Kaminski[1], Maor Sauler[1], Lieping Chen[7,8], Jin Woo Song[3]*, Tae Kon Kim[2]*, and Min-Jong Kang[1]*

[1]Section of Pulmonary, Critical Care, and Sleep Medicine, [5]Section of Rheumatology, Allergy, and Immunology, Department of Internal Medicine, [4]Department of Orthopedics and Rehabilitation, [6]Department of Pathology, [7]Department of Immunobiology, and [8]Yale Cancer Center, Yale University School of Medicine, New Haven, Connecticut; [2]Division of Hematology and Oncology, Department of Medicine at Vanderbilt University Medical Center, Nashville, Tennessee; and [3]Department of Pulmonary and Critical Care Medicine, Asan Medical Center, University of Ulsan College of Medicine, Seoul, Republic of Korea

ORCID IDs: 0000-0001-5917-4601 (N.K.); 0000-0003-3245-144X (M.-J.K.).

Abstract

VISTA (V domain immunoglobulin suppressor of T cell activation, also called PD-1H [programmed death-1 homolog]), a novel immune regulator expressed on myeloid and T lymphocyte lineages, is upregulated in mouse and human idiopathic pulmonary fibrosis (IPF). However, the significance of VISTA and its therapeutic potential in regulating IPF has yet to be defined. To determine the role of VISTA and its therapeutic potential in IPF, the expression profile of VISTA was evaluated from human single-cell RNA sequencing data (IPF Cell Atlas). Inflammatory response and lung fibrosis were assessed in bleomycin-induced experimental pulmonary fibrosis models in VISTA-deficient mice compared with wild-type littermates. In addition, these outcomes were evaluated after VISTA agonistic antibody treatment in the wild-type pulmonary fibrosis mice. VISTA expression was increased in lung tissue–infiltrating monocytes of patients with IPF. VISTA was induced in the myeloid population, mainly circulating monocyte-derived macrophages, during bleomycin-induced pulmonary fibrosis. Genetic ablation of VISTA drastically promoted pulmonary fibrosis, and bleomycin-induced fibroblast activation was dependent on the interaction between VISTA-expressing myeloid cells and fibroblasts. Treatment with VISTA agonistic antibody reduced fibrotic phenotypes accompanied by the suppression of lung innate immune and fibrotic mediators. In conclusion, these results suggest that VISTA upregulation in pulmonary fibrosis may be a compensatory mechanism to limit inflammation and fibrosis, and stimulation of VISTA signaling using VISTA agonists effectively limits the fibrotic innate immune landscape and consequent tissue fibrosis. Further studies are warranted to test VISTA as a novel therapeutic target for the IPF treatment.

Keywords: idiopathic pulmonary fibrosis; immune coinhibitory molecule; tissue fibrosis; VISTA; PD-1H

(Received in original form May 25, 2022; accepted in final form November 30, 2022)

*Co–Senior authors.

Supported by the Basic Science Research Program of the National Research Foundation, Republic of Korea, grant NRF-2022R1A2B5B02001602 (J.W.S.); American Society of Hematology Scholar Award 17-001379 (T.K.K.); the Edward P. Evans Foundation EvansMDS Young Investigator Award 18-003903 (T.K.K.); Concur Cancer Foundation American Society of Clinical Oncology Career Development Award 18-002055 (T.K.K.); American Cancer Society Clinician Scientist Development Award CSDG-18-198-01-LIB (T.K.K.); National Heart, Lung, and Blood Institute grant 1R01HL130283 (M.-J.K.); and National Institute on Aging grants 1R01AG053495 (M.-J.K.) and 1R56AG053495-06 (M.J.K.). The research reported/outlined here was supported by the Department of Veterans Affairs, Veterans Health Administration, VISN 1 Career Development Award to Edward Manning (E.M.). E.M. is a Pepper Scholar with support from the Claude D. Pepper Older Americans Independence Center at Yale School of Medicine (P30AG021342), NIA R03AG074063-01A1, and additional ventures.

Author Contributions: Conceived the idea and designed the experiments: S.-H.K., J.W.S., T.K.K., and M.-J.K.; performed experiments: S.-H.K., G.C., S.E.L., T.S.A., H.J.S., H.-K.K., H.-J.P., and E.M.; provided important reagents/tools: Q.H., F.Y.L., N.K., M.S., and L.C.; provided scientific insight: S.-H.K., H.-K.K., L.S., W.J.H., J.W.S., T.K.K., and M.-J.K.; analyzed data: S.-H.K., T.S.A., J.W.S., T.K.K., and M.-J.K.; drafted the manuscript: S.-H.K., J.W.S., T.K.K., and M.-J.K.; reviewed the manuscript: all authors.

Correspondence and requests for reprints should be addressed to Min-Jong Kang, M.D., Ph.D., Int Med – Pulmonary, Yale University School of Medicine, New Haven, CT 06520-8057. E-mail: min-jong.kang@yale.edu.

This article has a data supplement, which is accessible from this issue's table of contents at www.atsjournals.org.

Am J Respir Cell Mol Biol Vol 69, Iss 1, pp 22–33, July 2023

Originally Published in Press as DOI: 10.1165/rcmb.2022-0219OC on November 30, 2022
Internet address: www.atsjournals.org

Clinical Relevance

Immune dysregulation has emerged as a critical driver of idiopathic pulmonary fibrosis pathobiology. This study demonstrates that VISTA (V domain immunoglobulin suppressor of T cell activation), a novel immune coinhibitory molecule, is upregulated during the development of pulmonary fibrosis, wherein the fibrotic innate immune landscape and the consequent tissue fibrosis are enhanced in VISTA deficiency. Importantly, by demonstrating that agonistic VISTA antibody treatment can limit these responses, the current study provides proof-of-concept evidence that regulating innate immunity by stimulating VISTA can be an effective therapeutic strategy to limit lung fibrosis.

Idiopathic pulmonary fibrosis (IPF) is the most common type of fibrotic lung disorder. IPF confers a poor prognosis; the estimated median survival is only 2–5 years from the time of diagnosis (1, 2). Currently, two drugs—nintedanib and pirfenidone—are approved for IPF by the U.S. Food and Drug Administration. These drugs, however, provide only limited benefits as measured by life expectancy and their toxicities (2–4). Thus, there is a major unmet need to find novel therapies that can provide a survival benefit in IPF (5, 6).

Recent advances in our understanding of the role of the immune system in IPF indicate immune dysregulation as a critical driver of disease pathobiology (7). The significance of immune coinhibitory molecules in the pathogenesis of fibrotic lung diseases has also been proposed. For instance, serum amounts of CTLA-4 (cytotoxic T lymphocyte–associated protein 4) were elevated in patients with systemic sclerosis, which often causes pulmonary fibrosis, and correlated with disease severity and activity (8). Administration of anti–T cell immunoglobulin domain and mucin domain-3 monoclonal antibody (mAb) has been shown to exacerbate pulmonary inflammation and fibrosis in a bleomycin-induced murine model (9). More recently, the role of PD-1 (programmed cell death protein 1) and its ligand, PD-L1 (programmed death-ligand 1), in regulating lung fibrosis has been studied (10–12). In IPF lungs, PD-1–expressing T helper 17 cells were increased (10), and PD-1–null mice or use of antibody against PD-L1 demonstrated significantly reduced fibrosis compared with control mice after bleomycin injury, suggesting a pathogenic role of the PD-1/PD-L1 pathway in IPF (10). In contrast, another study suggested the protective role of PD-1/PD-L1 in IPF by demonstrating that human mesenchymal stem cells can alleviate pulmonary fibrosis in a PD-1/PD-L1 pathway–dependent manner (11). Despite multiple preclinical studies to examine the relationship between coinhibitory molecules and IPF, targeting coinhibitory molecules for the treatment of IPF and its clinical application is far from established (13).

VISTA (V domain immunoglobulin suppressor of T cell activation, also called PD-1H [programmed death-1 homolog]) is a novel immune checkpoint protein that belongs to the B7/CD28 gene family (14, 15) that is predominantly expressed in hematopoietic cells. VISTA regulates inflammation and maintains T cell tolerance (16), and VISTA agonism inhibits autoimmune diseases by suppressing the activation of T cells and neutrophils in several murine models (17–19). Importantly, VISTA is most prominently expressed in the lungs, bone marrow, and spleen, with lower expression in many other organs including the thymus, liver, heart, brain, and kidney (14). The role of VISTA in pulmonary fibrosis, however, has yet to be defined.

Here, we demonstrate that VISTA, upregulated primarily in lung monocytes/macrophages during the development of pulmonary fibrosis, limits the fibrotic innate immune landscape and the consequent tissue remodeling responses. We also demonstrate the therapeutic potential of VISTA by assessing clinical outcomes in a mouse model after treatment with a VISTA agonist.

Methods

Human Single-Cell RNA Sequencing Reanalysis

Previously reported single-cell RNA sequencing (scRNAseq) data (20) representing 32 IPF and 28 control lungs were downloaded from the Gene Expression Omnibus repository, accession no. GSE136831. Data were analyzed in R (RStudio) using the package Seurat. Samples from patients with chronic obstructive pulmonary disease and cells labeled as multiplets were removed. Unique molecular identifier counts were normalized to 10,000 transcripts per cell, then log normalized with a pseudocount of one. All cell-type labels shown correspond to what was previously reported.

To generate a uniform manifold approximation and projection (UMAP) of all cells, the top 2,250 genes were selected based on the default parameters of Seurat's FindVariableFeatures implementation and used for principal component (PC) analysis. PCs 1–11 and 15–22 were then selected for UMAP plotting; PCs 12–14 were avoided because their gene loading correlates were associated with either cell-cycle or mitochondrial genes. Selected PCs were used with Seurat's RunUMAP implementation with 60 nearest neighbors, a local connectivity of 5, a minimum distance of 0.25, and a spread value of 1.5 for 200 iterations with the random seed 7.

To generate the UMAP of classical and nonclassical monocytes, the top 2,000 genes were selected based on the default parameters of Seurat's FindVariableFeatures implementation. We then regressed out signals associated with scaled mitochondrial RNA expression using the vars.to.regress argument in Seurat's ScaleData implementation for subsequent use in PC analysis. PCs 1–7 were used with Seurat's RunUMAP implementation with 30 nearest neighbors, a local connectivity of 3, a minimum distance of 0.3, and a spread value of 1.3 for 2,000 iterations with a learning rate of 0.8 and random seed 7.

Mice and Experimental Pulmonary Fibrosis

Vista knockout ($^{-/-}$, KO) mice (GenBank gene NM_028732; GenBank protein JN602184) were purchased from the Mutant Mouse Regional Resource Center (University of California Davis) as previously described (21). Wild-type (WT) C57BL/6N from Charles River Laboratories and *Vista* KO mice were all kept on a C57BL/6N background and bred at the Yale University Animal Facility. To induce pulmonary fibrosis that is significant but not lethal in *Vista* KO mice, we administered bleomycin (0.8 U/kg, NDC 61703-0332-18; Pfizer) for WT C57BL/6N and *Vista* KO mice, respectively, by intratracheal administration

following the methodology previously described by our laboratory (22). For the VISTA agonistic mAb experiment, WT C57BL/6J mice were purchased from Jackson Laboratory, and the dose of 0.4 U/kg of the same bleomycin was administered to induce similar levels of pulmonary fibrosis observed from WT C57BL/6N mice. The VISTA agonistic mAb was produced and purified as previously described (15). At indicated time points after bleomycin administration, mice were killed, and lungs were harvested for further analyses. All animal experiments were approved by the Yale Animal Care and Use Committee.

Statistics

Statistical analysis was performed with GraphPad Prism (version 8). Comparisons between two groups were performed with Student's *t* test (unpaired). For multiple comparisons, one- or two-way ANOVA was used. Values are expressed as mean ± SEM. Statistical significance was defined at P values < 0.05.

Specific descriptions of the methods are provided in the data supplement.

Results

VISTA Is Upregulated in Pulmonary Monocyte-derived Alveolar Macrophages from Patients with IPF

Although the role of immune coinhibitory molecules in the regulation of fibrotic lung diseases has recently been studied, the role of VISTA in regulating pulmonary fibrosis has yet to be defined. As an initial step to address this issue, we evaluated the VISTA expression profile in lungs from patients with IPF. Specifically, after the classification of 38 discrete cell types identified from our recently reported human scRNAseq data (20, 23), we reevaluated the profile of UMAP representing 292,462 cells from 32 IPF and 28 control lungs (Figure 1A). Across the 38 cell types annotated, we observed the highest average VISTA expression among nonclassical (ncMonocytes) and classical monocytes (cMonocytes) (0.881, 0.768 log[(TPM/100) + 1], respectively), followed by conventional dendritic cells (type I and II), mature dendritic cells, and fibroblasts (Figure 1B). VISTA expression was rarely observed in type I and II airway epithelial cells (Figure 1B). We then further explored VISTA expression patterns between disease and control subsets, and the UMAP profile revealed a distinct separation between the groups (Figure 1C). We observed elevated VISTA expression in both cMonocytes and ncMonocytes from subjects with IPF (Figure 1D) and across subjects (Figure 1E). A recent human scRNAseq study of patients with IPF (IPF Cell Atlas, www.ipfcellatlas.com) has shown the existence of at least six distinct subpopulations in pulmonary macrophages (23). Interestingly, among these subpopulations, both cMonocytes and ncMonocytes have shown prominent expression of VISTA, whereas others rarely expressed VISTA (*see* Figure E1A in the data supplement). The literature has demonstrated that cMonocytes and ncMonocytes are found in all lungs irrespective of disease state (24, 25), indicating that these subpopulations (cMonocytes and ncMonocytes) of pulmonary macrophages can be regarded as monocyte-derived alveolar macrophages. It should be noted that the expression pattern of VISTA in immune cell populations was distinct from those of other immune checkpoint molecules such as PD-1, PD-L1, CTLA-4, and hepatitis A virus cellular receptor 2 (TIM3) (Figure E1). Among these immune checkpoint molecules, VISTA was unique in that the expression was most highly upregulated in monocyte-derived alveolar macrophages, whereas others were more abundantly observed in lymphoid lineage cells from patients with IPF (Figure E1B).

VISTA Is Induced in Pulmonary Tissue-Infiltrating Monocyte-derived Alveolar Macrophages during Bleomycin Injury

Next, to determine the regulation of VISTA expression during the development of experimental pulmonary fibrosis, we used a well-established murine model of bleomycin-induced pulmonary fibrosis as described in our recent publication (22). The expression of VISTA, in addition to other immune checkpoint molecules, was significantly increased and peaked at Day 14 after bleomycin, which is typically regarded as the fibrogenic phase after bleomycin injury (Figures 2A and E2A). The increased VISTA expression persisted at Day 21 after bleomycin (Figures 2A and 2C). BAL fluid, which mainly contains immune cells, revealed a significant increase of VISTA expression at Day 14 after bleomycin administration (Figure 2B). In agreement with the fibrotic phase, the levels of αSMA (α-smooth muscle actin) and fibronectin increased significantly by Day 14 (Figures 2C and E2B). VISTA upregulation in murine fibrotic lung tissue relied on the infiltration of monocytes/macrophages (Figure 2C). Immunofluorescence staining showed colocalized VISTA expression in cells of the monocyte/macrophage lineage expressing CD14 (Figure 2D). The specificity of VISTA staining in our experiments was verified by the absence of a staining signal in *Vista* KO mice (Figures E2C–E2E). Flow cytometric analysis revealed a similar result. Specifically, from the whole lung cells obtained at Day 14 after bleomycin injury *in vivo*, we prepared whole lung single-cell suspensions following the methodology reported in our study (26). Then, when we evaluated the levels of VISTA expression in various $CD45^+$ hematopoietic cells, the VISTA expression was mainly observed from $F4/80^+$ macrophages; then $CD3^+$ T cells and other immune cells followed (Figure 2E). To identify the subsets of the pulmonary macrophage population expressing VISTA, we isolated interstitial macrophages, monocyte-derived alveolar macrophages (Mo-AM), and tissue-resident alveolar macrophages and analyzed the expression of VISTA by flow cytometry. As reported previously (27, 28), alveolar macrophages were reconstituted with Mo-AM after bleomycin injury (Figure E2F). Consistent with the frequency of Mo-AM, VISTA expression was highest in this population in post-bleomycin fibrotic lung tissue, although VISTA is equivalently expressed on other subtypes of macrophages (Figures 2F and E2G).

VISTA Regulates Bleomycin-induced Lung Injury via Innate Immunity

To define the role of VISTA in the regulation of lung fibrosis, bleomycin-induced fibrotic severity was assessed in the lungs of C57BL/6N $Vista^{-/-}$ or littermate WT control mice. Bleomycin administration resulted in lung fibrosis as measured by deposition of collagen content and fibrotic pathology scores in the lung tissues at Day 14. Interestingly, the bleomycin-induced tissue fibrosis was markedly enhanced in lungs of $Vista^{-/-}$ mice (Figures 3A and 3B). The enhanced pulmonary fibrosis in $Vista^{-/-}$ mice was further confirmed at Day 21 after bleomycin by the measurement of lung total collagen content using a Sircol assay (Figure 3C). The increased fibrosis in *Vista* KO mice was associated with higher levels of activated TGF-β1 (transforming growth factor β-1), a prominent profibrotic

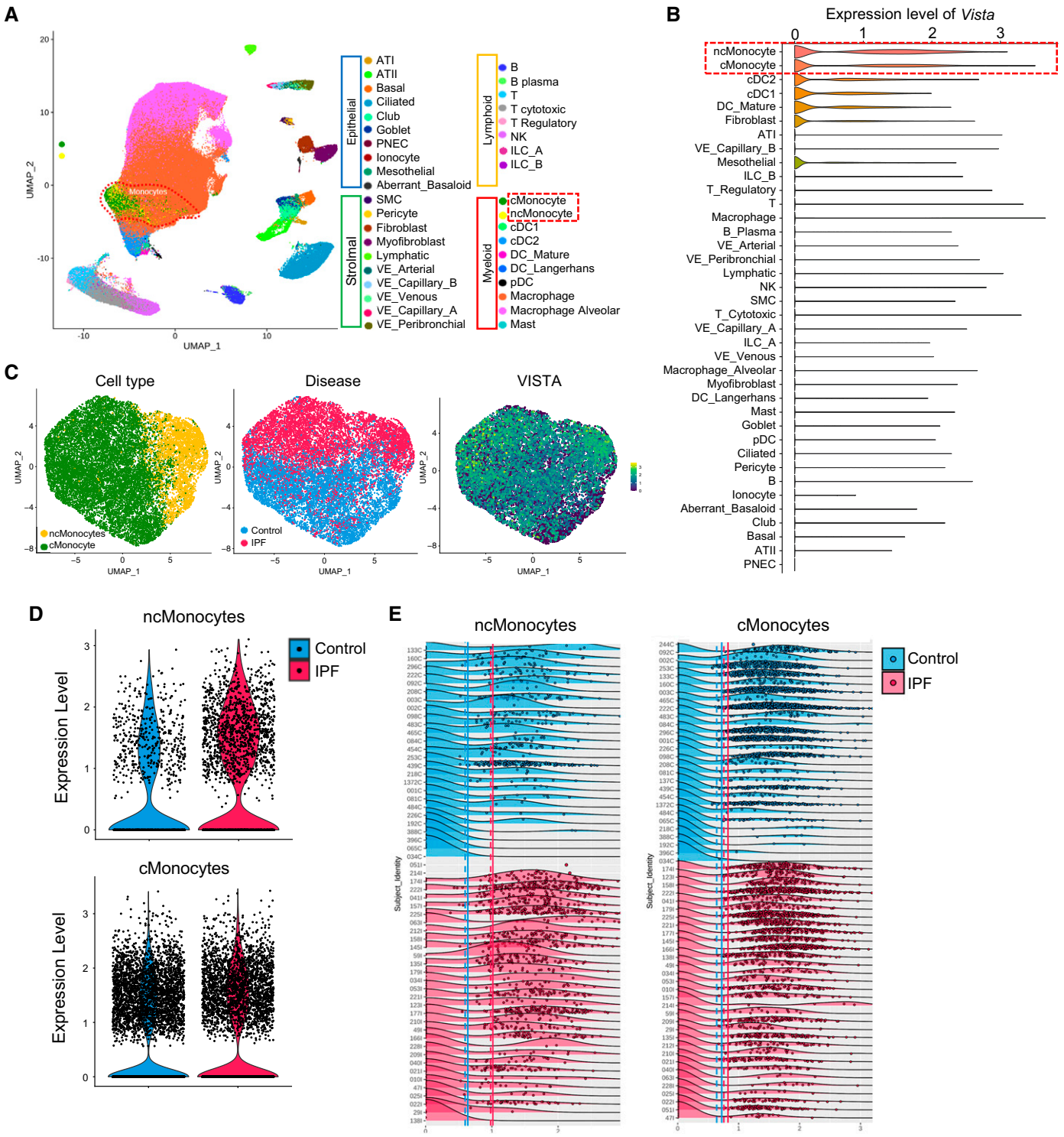

Figure 1. VISTA (V domain immunoglobulin suppressor of T cell activation) expression is increased in monocyte-derived macrophages (classical [cMonocytes] and nonclassical [ncMonocytes]) of lungs from patients with idiopathic pulmonary fibrosis (IPF). (*A*) Uniform manifold approximation and projection (UMAP) of 243,472 cells obtained from 28 healthy control lungs and 32 lungs from subjects with IPF. Cells are labeled by cell type. (*B*) Violin plots representing the distribution of normalized VISTA expression across different cell types from IPF and control lungs. Cell types are in descending order of average normalized VISTA expression. (*C*) UMAPs of 13,957 ncMonocytes and cMonocytes from 28 healthy control subjects and 32 patients with IPF, labeled by cell type, disease, and VISTA expression. (*D*) Violin plots of expression of VISTA across ncMonocytes and cMonocytes from control and IPF lungs. (*E*) Density plots of normalized VISTA expression among either ncMonocytes and cMonocytes across samples of IPF and control lungs. Samples are grouped by disease, then ordered by average cell VISTA expression. Each dot represents one cell; each treatment's solid and dashed vertical lines correspond to mean cell and mean subject VISTA expression, respectively. AT = alveolar type; cDC = classical dendritic cell; ILC = innate lymphoid cell; NK = natural killer; pDC = plasmacytoid dendritic cell; PNEC = pulmonary neuroendocrine cell; VE = vascular endothelial.

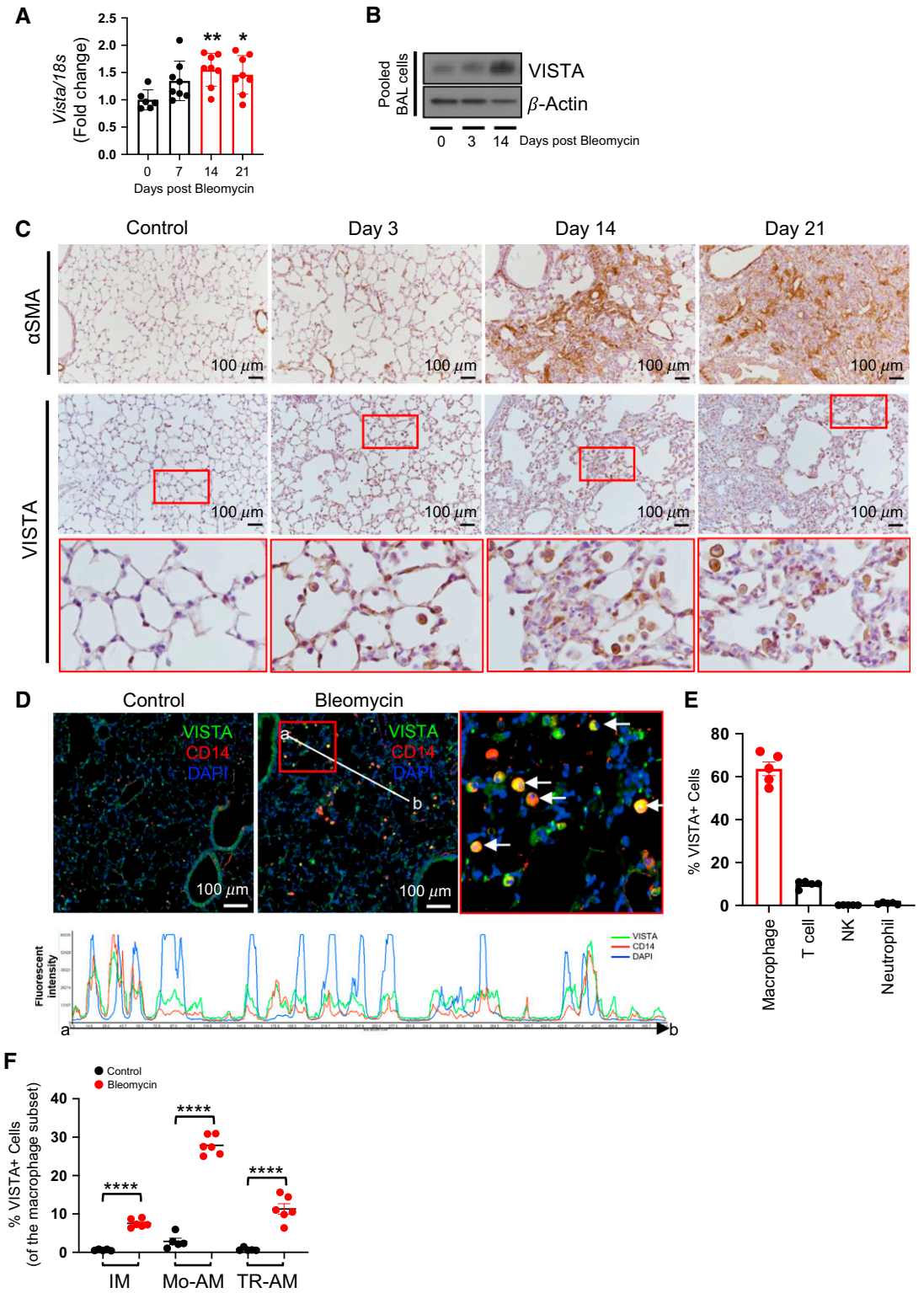

Figure 2. VISTA is expressed in monocyte-derived macrophages during lung fibrosis after bleomycin administration *in vivo.* C57BL/6 mice were injected with saline (−) or 0.4 U/kg of bleomycin (+) intratracheally. (*A*) The expression levels of *Vista* mRNAs were evaluated from whole lung tissues at indicated time points after bleomycin administration by qRT-PCR. Expression was normalized to 18S mRNA. (*B*) Alveolar macrophages were isolated and pooled at Days 3 and 14 after bleomycin administration ($n = 5$ per group). Then, the expression of VISTA was evaluated by Western blot analysis. β-actin was used as a loading control. (*C*) Representative images from immunohistochemical analysis of α-SMA (α-smooth muscle actin) and VISTA staining of lung sections at Days 3, 14, and 21 after bleomycin administration ($n = 5$ per group).

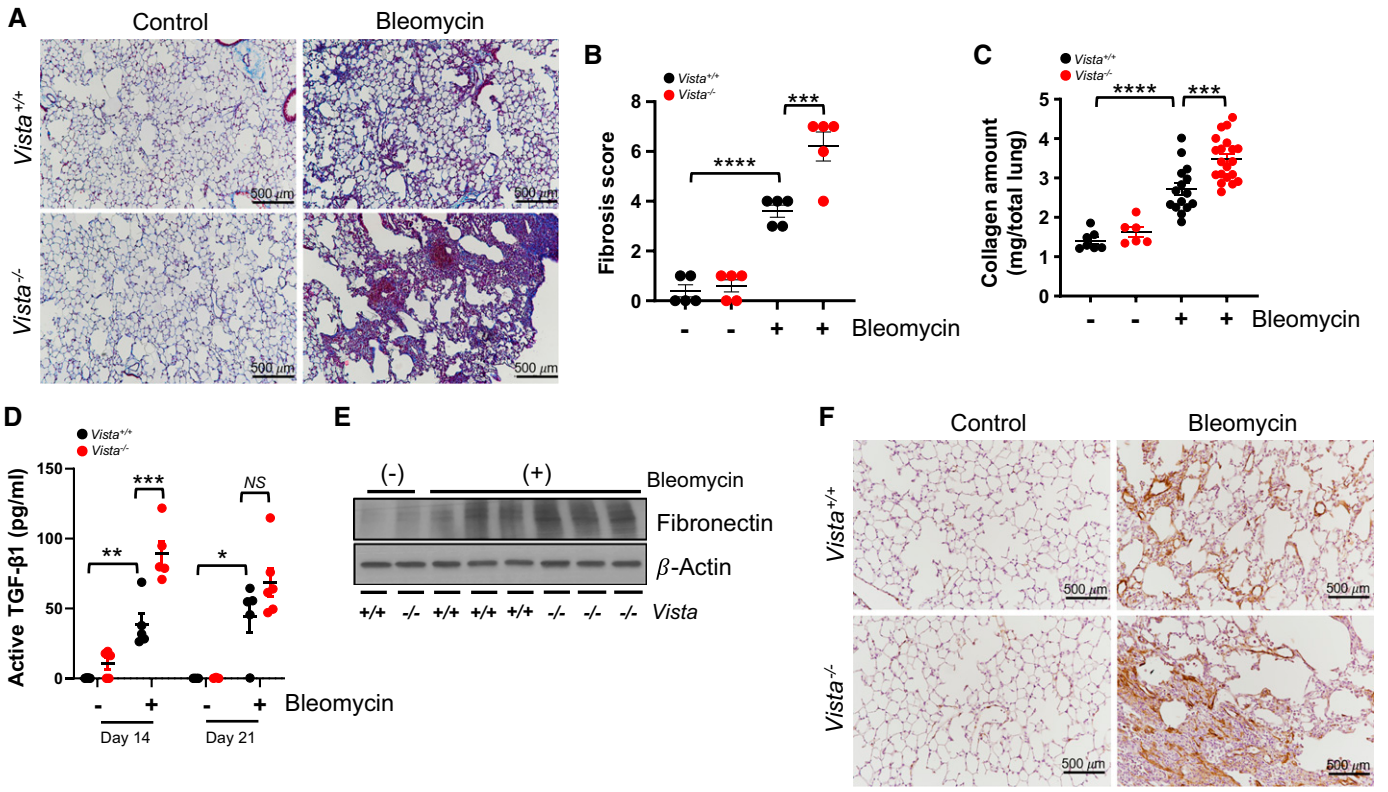

Figure 3. Bleomycin-induced fibrosis is aggravated in *Vista*$^{-/-}$ mice. *Vista*$^{-/-}$ mice or wild-type (WT) control mice (*Vista*$^{+/+}$) were injected with saline (bleomycin −) or 0.8 U/kg of bleomycin (+) intratracheally. (*A*) Representative Masson's trichrome staining of lung sections and (*B*) fibrosis score from *Vista*$^{+/+}$ or *Vista*$^{-/-}$ mice at Day 14 after bleomycin administration ($n = 5$ per group). (*C*) Collagen content of total lung tissues at Day 21 after bleomycin administration ($n = 6$–7 per saline group and $n = 15$–20 per bleomycin group). (*D*) Active TGF-β1 (transforming growth factor β-1) levels at Days 14 and 21 after bleomycin administration were measured from the BAL fluid by ELISA ($n = 4$–5 per saline group and $n = 5$–6 per bleomycin group). (*E*) Western blot of fibronectin in lung homogenates of bleomycin-induced *Vista*$^{+/+}$ or *Vista*$^{-/-}$ mice. β-actin was used as a loading control. (*F*) Representative images from immunohistochemical analysis of αSMA in lung sections at Day 14 after bleomycin administration ($n = 5$ per group). Scale bars, 500 μm. Data are mean ± SEM. Statistical significance was determined using one-way ANOVA with Tukey's multiple comparisons test. *$P < 0.05$, **$P < 0.01$, ***$P < 0.001$, and ****$P < 0.0001$. NS = not significant.

mediator (Figure 3D), together with elevated levels of fibronectin (Figures 3E and E3A) and staining of αSMA, an important marker of myofibroblast activation (Figure 3F). These results demonstrate that VISTA negatively regulates the fibrotic response in lungs after bleomycin injury.

Consistent with our data demonstrating the increased infiltration of VISTA-expressing Mo-AM in post-bleomycin fibrotic lung (Figure 2F), bleomycin administration led to a more significant accumulation of inflammatory cells in the BAL fluids of VISTA$^{-/-}$ mice compared with those of WT mice at Day 14 after bleomycin administration (Figure 4A). At this point, cytokines and chemokines associated with human IPF, as determined by WebGestalt (Web-based GEne SeT AnaLysis Toolkit), were significantly elevated in *Vista*$^{-/-}$ mice after bleomycin (Figures 4B and E3B–E3D). These data suggest that VISTA$^{-/-}$ is one of the key inhibitory regulators of IPF and that this regulation was executed by innate immunity. In addition, we found enhanced production of danger-associated molecular patterns, such as mitochondrial TFAM (transcription factor A) and HMGB1 (high-mobility group box 1), in *Vista*$^{-/-}$ lungs (Figure 4C) at the time point

Figure 2. (*Continued*). The red boxed region was magnified in the images below. Scale bars, 100 μm. (*D*) Representative images from the immunofluorescence analysis of VISTA (green) in lung sections at Day 14 after bleomycin or PBS administration ($n = 5$ per group). CD14 antibody (red) was used for the immunofluorescence staining of monocytes/macrophages. The red boxed region is magnified for closer observation. White arrows point to colocalization of VISTA and CD14 in lung cells. Histogram of the fluorescence intensity evaluated from the interval (point a–b) shows colocalization of VISTA and CD14 cells. Nuclei were counterstained with DAPI. Scale bars, 100 μm. (*E*) The percentage of each immune cell subpopulation (gated on CD45$^+$ cells) among the VISTA-expressing cells from bleomycin-administered lungs at Day 14 was determined by flow cytometry ($n = 5$). (*F*) FACS analysis of different macrophage populations showed the frequency of VISTA expression ($n = 5$ per control group and $n = 6$ per bleomycin group). Data are mean ± SEM. Statistical significance was determined using two-way ANOVA with Tukey's multiple comparisons test. *$P < 0.05$, **$P < 0.01$, and ****$P < 0.0001$. IM = interstitial macrophages; Mo-AM = monocyte-derived alveolar macrophages; TR-AM = tissue-resident alveolar macrophages.

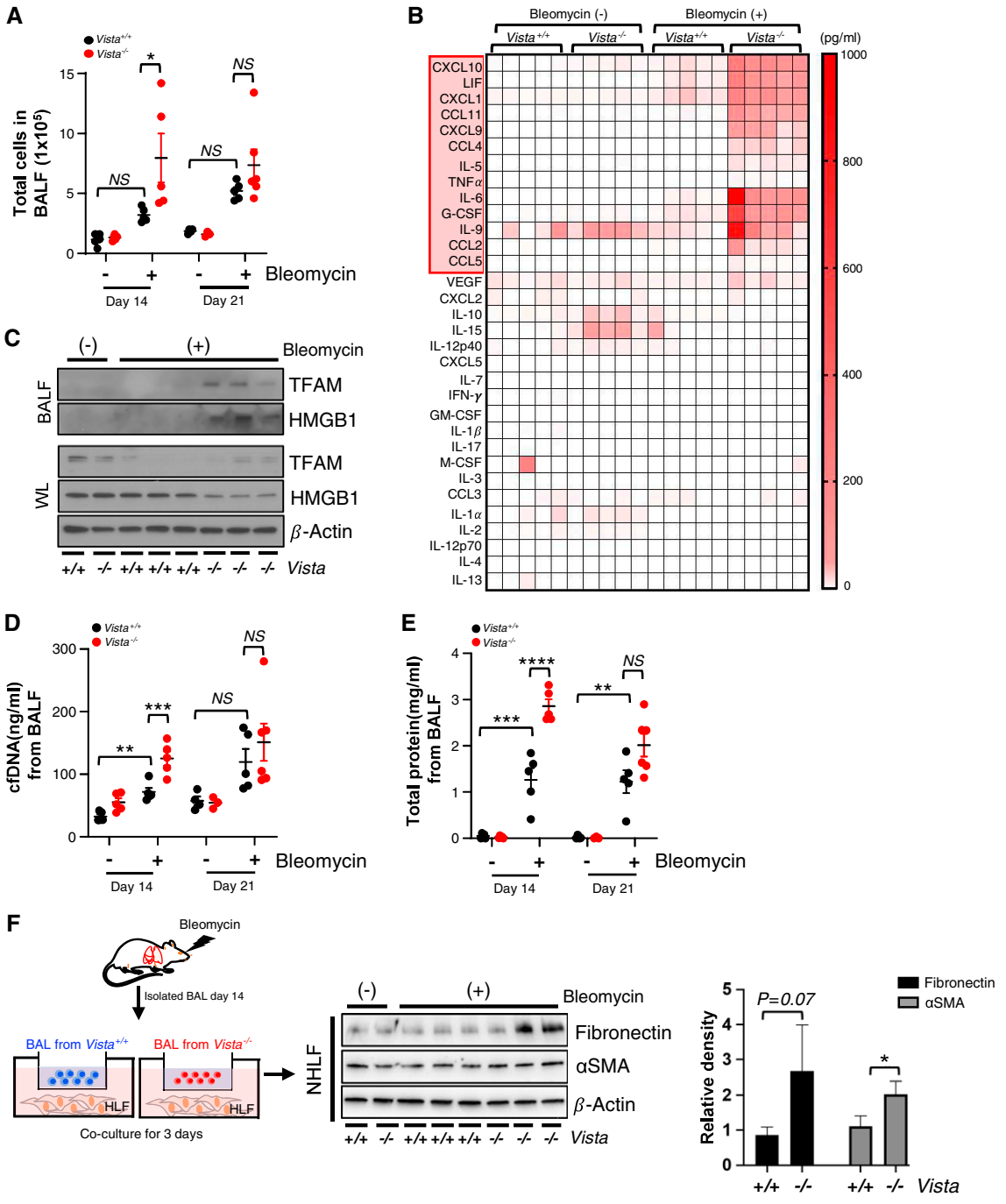

Figure 4. Bleomycin-induced fibrotic immune and inflammatory responses are aggravated in *Vista*$^{-/-}$ mice. *VISTA* knockout (*Vista*$^{-/-}$) mice or WT controls (*Vista*$^{+/+}$) were injected with saline (bleomycin −) or 0.8 U/kg of bleomycin (+) intratracheally. (*A*) Total cell counts at Days 14 and 21 after bleomycin administration were evaluated from the BAL fluid (BALF) ($n = 4$–5 per saline group and $n = 5$–6 per bleomycin group). (*B*) Cytokine and chemokine concentrations at Day 14 after bleomycin administration were measured from the BALF by multiplex ELISA ($n = 5$ per group). (*C*) Western blot of HMGB1 (high-mobility group box 1) and TFAM (transcription factor A) from BALF and whole lysates (WL) of bleomycin-induced *Vista*$^{+/+}$ or *Vista*$^{-/-}$ mice. β-actin was used as a loading control. (*D*) The amount of cell-free DNA (cfDNA) in BALF at Days 14 and 21 after bleomycin administration was evaluated by fluorometric assays ($n = 4$–5 per saline group and $n = 5$–6 per bleomycin group). (*E*) Total protein concentration in BALF at Days 14 and 21 after bleomycin administration ($n = 4$–5 per saline group and $n = 5$–6 per bleomycin group). (*F*) BAL cells isolated from *Vista*$^{+/+}$ or *Vista*$^{-/-}$ mice at Day 14 after bleomycin were incubated with normal human lung fibroblasts (NHLF) for 3 days and then the cell lysates were obtained. (*G*) The levels of fibronectin and αSMA in NHLF media. Representative images and densiometric quantification are shown ($n = 3$ per group). Data are mean ± SEM. Statistical significance was determined using one-way ANOVA with Tukey's multiple comparisons test. *$P < 0.05$, **$P < 0.01$, ***$P < 0.001$, and ****$P < 0.0001$. G-CSF = granulocyte colony stimulating factor; GM-CSF = granulocyte-macrophage colony-stimulating factor; LIF = leukemia inhibitory factor; M-CSF = colony stimulating factor 1; VEGF = vascular endothelial growth factor.

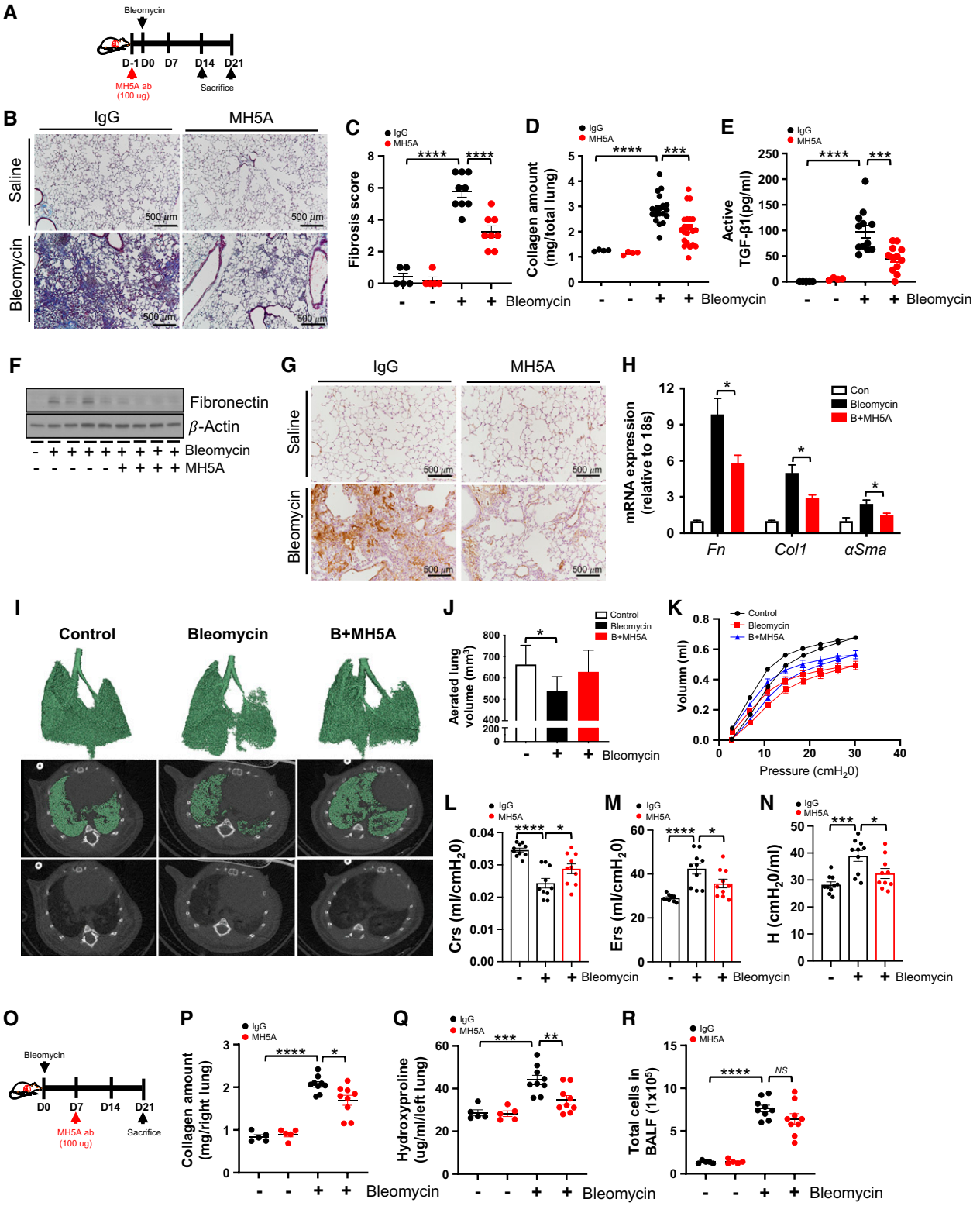

Figure 5. Agonistic VISTA antibody attenuates bleomycin-induced fibrosis. (*A*) A schematic diagram for the administration of MH5A or control IgG in bleomycin-induced lung fibrosis. MH5A (100 μg) was injected intraperitoneally on Day 1 (D1) before bleomycin administration, and lungs were assessed at Days 14 and 21 after bleomycin administration. (*B* and *C*) Representative Masson's trichrome staining of (*B*) lung sections and (*C*) fibrosis score from MH5A- or IgG-treated mice at Day 14 after bleomycin administration ($n = 5$ per saline group and $n = 8$–9 per bleomycin group). Scale bars, 500 μm. (*D*) Collagen content of total lung tissues at Day 21 after bleomycin administration ($n = 4$ per saline group and $n = 19$–22 per bleomycin group).

of Day 14 after bleomycin administration. Interestingly, we also observed enhanced levels of cell-free DNAs and total protein amounts in the BAL samples of *Vista*$^{-/-}$ mice at Day 14 after bleomycin administration (Figures 4D and 4E). However, these values of total cell recovery, cell-free DNAs, and total protein amounts in the BAL samples showed an increased tendency but were not statistically different at Day 21 after bleomycin administration. Taken together, these also support that VISTA-mediated regulation of pulmonary fibrosis is associated with innate immune/inflammatory responses. To determine whether VISTA-expressing immune cells can limit the activation of human fibroblasts, although recognizing the difference in species specificity, we cocultured the BAL cells from *Vista*$^{-/-}$ or WT mice after bleomycin with normal human lung fibroblasts in Transwell chambers as indicated in Figure 4F. Interestingly, VISTA-deficient cells significantly upregulated fibronectin and αSMA in the normal human lung fibroblasts (Figure 4G), further confirming the role of VISTA in limiting the fibrotic response.

VISTA Agonism Attenuates the Severity of Experimental Lung Fibrosis

Given the role of VISTA in negative regulation of pulmonary fibrosis, we determined whether stimulating VISTA-mediated signaling could inhibit lung fibrosis using a VISTA agonistic mAb (clone: MH5A) (15). For these experiments, C57BL/6J WT mice were used. We administered MH5A or control mIgG on Day 1 before bleomycin injury as illustrated in Figure 5A. The pretreatment with MH5A prevented lung fibrosis based on a significant reduction in the collagen content and fibrotic scores in the lungs at Day 21 after bleomycin (Figures 5B–5D). The decreased lung fibrosis was associated with decreases in active TGF-β1, fibronectin, and αSMA in the lungs (Figures 5E–5G). Furthermore, mRNA levels of collagen 1α, fibronectin, and αSMA were significantly decreased upon treatment with MH5A (Figure 5H).

To further determine the detailed impact of VISTA agonism, we performed micro–computed tomography (micro-CT) analysis of bleomycin-exposed mouse lung with or without MH5A treatment. Micro-CT data showed that bleomycin significantly decreased aerated lung volume, which was partially restored using MH5A treatment. This is shown by three-dimensional reconstruction images of micro-CT scans and aerated lung volume (Figures 5I and 5J). In addition, pulmonary function tests were performed to quantify further the effects of MH5A treatment on the total respiratory system and lung parenchyma in bleomycin-induced fibrotic lungs. Indeed, MH5A treatment recovered various mechanical properties of the respiratory system, including pressure/volume loop curve, dynamic compliance, dynamic elasticity, and tissue elastance after bleomycin-induced injury (Figures 5K–5N). Collectively, our data suggest that VISTA agonism attenuates post-bleomycin lung fibrosis.

To determine if VISTA agonism reverses established post-bleomycin fibrotic injury, we started the treatment at Day 7 after bleomycin administration (Figure 5O). Indeed, the MH5A therapy at Day 7 after bleomycin administration significantly attenuated lung fibrosis (Figures 5P and 5Q), although its effects on pulmonary inflammation showed a decreased tendency but were not statistically significant (Figure 5R). We also obtained a similar significant attenuation of lung fibrosis when we administered MH5A at Day 3 after bleomycin administration (Figures E4A and E4B). Collectively, these suggest that administering MH5A after bleomycin exposure can provide therapeutic benefits against the development of pulmonary fibrosis.

The VISTA Agonist Limits Innate Immunity in Experimental Pulmonary Fibrosis

Consistent with improvement of fibrosis upon treatment with MH5A, the bleomycin injury–induced upregulation of multiple innate immune/inflammatory cytokines and chemokines was significantly attenuated upon treatment with MH5A mAb (Figure 6A). Accompanied by the protein levels measured by the multiplex assay, mRNA expression was also significantly decreased for these innate immune mediators (Figure 6B), suggesting a persistent effect of VISTA agonism on these cytokine responses. In addition, the expression levels of multiple genes known to contribute to the pathogenesis of fibrosis were significantly reduced after MH5A treatment (Figure E5). Consistent with the above, MH5A significantly decreased the total number of inflammatory cells, levels of cell-free DNA, and total protein in the BAL fluid at Day 14 after bleomycin (Figures 6C–6E).

Discussion

In the current study, we demonstrated that *1*) VISTA is upregulated in both murine and human lung cells during the development of

Figure 5. (*Continued*). (*E*) Active TGF-β1 levels at Day 14 after bleomycin administration were measured from the BALF by ELISA ($n = 4$–5 per saline group and $n = 12$ per bleomycin group). (*F*) Western blot of fibronectin in lung homogenates of MH5A- or IgG-treated mice at Day 14 after bleomycin administration. β-actin was used as a loading control. (*G*) Representative images from immunohistochemistry analysis of αSMA on lung sections at Day 21 after bleomycin administration are presented ($n = 5$ per group). Scale bars, 500 μm. (*H*) The expression levels of fibronectin (Fn), collagen 1α (Col1), and αSMA mRNAs were evaluated from whole lung tissues at Day 14 after bleomycin administration by qRT-PCR ($n = 10$ per group). Expression was normalized to 18S mRNA. (*I*) Representative three-dimensional reconstruction and micro–computed tomography (micro-CT) images of lung tissue at Day 21 after bleomycin administration. (*J*) Aerated lung volume was measured by quantitative CT renditions ($n = 5$ per group). (*K–N*) Lung function was determined at Day 21 after bleomycin administration by the flexiVent system ($n = 10$). (*K*) Pressure/volume loop curves, (*L*) Crs, (*M*) Ers, and (*N*) tissue elastance (*H*) are shown. (*O–R*) (*O*) A schematic diagram for the administration of MH5A or control IgG in bleomycin-induced lung fibrosis. MH5A (100 μg) was injected intraperitoneally on Day 7 after bleomycin administration, and lungs were assessed at Day 21 after bleomycin administration ($n = 5$ per saline group and $n = 9$ per bleomycin group). (*P*) Collagen content of right lung tissues at Day 21 after bleomycin administration. (*Q*) Hydroxyproline content of left lung tissues at Day 21 after bleomycin administration. (*R*) Total cell counts at Day 21 after bleomycin administration were evaluated from the BALF. Data are mean ± SEM. Statistical significance was determined using one-way ANOVA with Tukey's multiple comparisons test. $^{*}P < 0.05$, $^{**}P < 0.01$, $^{***}P < 0.001$, and $^{****}P < 0.0001$. B+MH5A = bleomycin plus MH5A; Crs = lung compliance; Ers = respiratory system elastance.

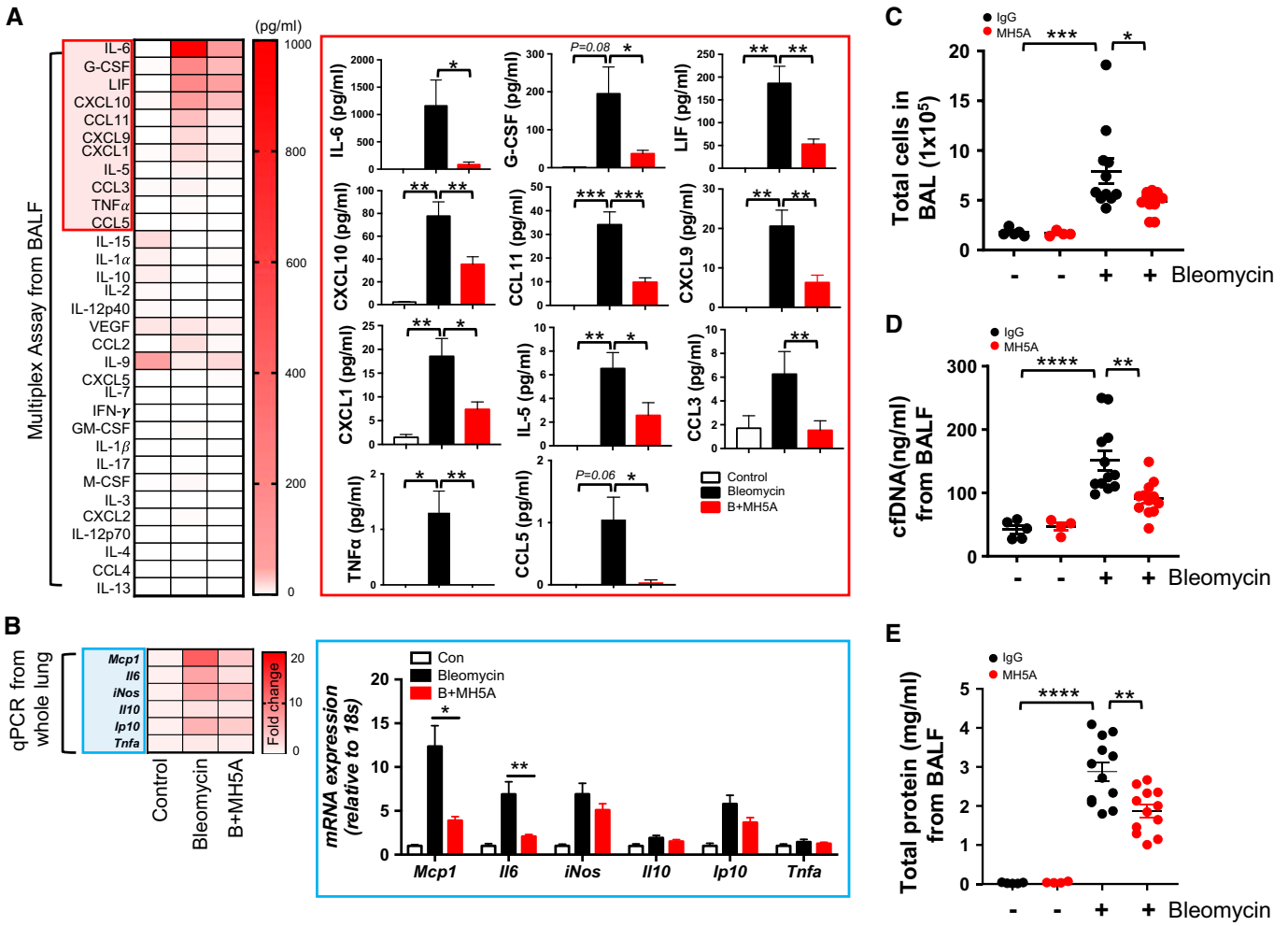

Figure 6. Agonistic VISTA antibody inhibits pathologic innate immune responses after bleomycin treatment. MH5A (100 μg) was injected intraperitoneally 1 day before bleomycin administration, and samples were collected at 14 days after bleomycin administration. (*A*) Cytokine and chemokine concentrations were measured from the BALF by multiplex ELISA ($n = 5$ per control and $n = 12$ per bleomycin group). (*B*) The expression levels of *Mcp1*, *Il6*, *iNOS*, *Il10*, *Ip10*, and *Tnfa* mRNAs were evaluated from whole lung tissues after bleomycin administration by qRT-PCR. (*C*) Total cell counts from BALF were evaluated ($n = 4$–5 per saline group and $n = 12$ per bleomycin group). (*D*) The amount of cfDNA was evaluated from BALF by fluorometric assays ($n = 4$–5 per saline group and $n = 12$ per bleomycin group). (*E*) Total protein concentration was evaluated from BALF ($n = 4$–5 per saline group and $n = 12$ per bleomycin group). Data are mean ± SEM. Statistical significance was determined using one-way ANOVA with Tukey's multiple comparisons test. *$P < 0.05$, **$P < 0.01$, ***$P < 0.001$, and ****$P < 0.0001$. C-C motif = chemokine; iNos = nitric oxide synthase 2; Mcp1 = ligand 2.

pulmonary fibrosis, and VISTA upregulation mostly results from infiltrated cells of myeloid origin (monocytes/macrophages); *2*) VISTA regulates post-bleomycin fibrotic lung injury via innate immunity; and *3*) stimulating VISTA signaling with an agonistic antibody improves the severity of fibrosis. Taken together, these findings provide proof-of-concept evidence that regulation of innate immunity by stimulating VISTA can be an effective therapeutic strategy to limit lung fibrosis.

IPF is a debilitating condition that often manifests at an advanced age. Throughout life, multiple exposures to noxious stimuli and microinjuries to lungs are believed to contribute to the pathogenesis of IPF, wherein the accumulated tissue injury/damage leads to aberrant repair processes resulting in extensive deposition of collagen in the lung (2, 29, 30). Although the host mechanisms that modulate the microinjuries and subsequent misdirected repair leading to fibrosis are still poorly understood, innate immune cells such as tissue-infiltrating macrophages and monocytes seem to constitute an essential arm of the host mechanisms that regulate lung fibrosis (20, 22, 27, 31). In addition, reprogramming of profibrotic macrophages has been shown to have therapeutic potential in experimental fibrosis (28). Hence, identifying such innate immune regulators that can inhibit fibrosis might provide the critical insights needed to develop therapeutic interventions for IPF. Interestingly, our human IPF Atlas data set revealed that VISTA, a novel immune coinhibitory molecule, is mainly expressed in cells of myeloid origin, including monocytes (cMonocytes and ncMonocytes) and dendritic cells, of subjects with IPF, whereas its expression is limited in lymphoid cells. The literature indicates that these subpopulations (cMonocytes and

ncMonocytes) of pulmonary macrophages can be regarded as monocyte-derived alveolar macrophages (24, 25). Indeed, the expression pattern of VISTA in our experimental pulmonary fibrosis model was similar to the human findings, showing the most prominent expression in tissue-infiltrating monocytes/macrophages. Importantly, our *in vivo* studies using an established experimental pulmonary fibrosis model reveal a previously undiscovered role of VISTA in limiting lung fibrosis. In line with this, recent studies highlight a crucial inhibitory role of VISTA in keeping the immune cells in a quiescent state during autoimmune or sepsis pathobiology (32, 33). Taken together, these observations enable us to speculate that VISTA expression may be upregulated on myeloid innate immune cells to negatively regulate fibrogenic immunity as a homeostatic response during aberrant tissue repair, and, thus, stimulating the tonic antifibrotic innate immunity by activating VISTA signaling could be an effective therapeutic approach to limit tissue fibrosis.

Recently, scientific advances have illuminated immune dysregulation as a crucial aspect of IPF pathobiology (7). In line with this, momentum is increasing to develop targeted immunomodulatory therapies that successfully halt or potentially even reverse lung fibrosis (7, 13). In this respect, immune checkpoint molecules such as CTLA-4, PD-1, and VISTA may offer such an opportunity to modulate fibrogenic immunity and the consequent lung fibrosis. Indeed, recent studies demonstrate these endeavors (9–13). VISTA is most prominently expressed in lungs and spleen (14). In addition, VISTA is one of the checkpoint molecules highly expressed in myeloid cells, whereas others are mainly expressed in lymphoid cells, conferring a unique opportunity to target pulmonary macrophages that play an essential role in IPF pathobiology. As such, VISTA modulation may have a distinct advantage for immunomodulation for lung diseases by targeting innate immunity, compared with other immune checkpoint molecules mainly expressed on T cells (32, 33). Currently, immunotherapy targeting coinhibitory molecules for the treatment of IPF is far from established (13), and the knowledge obtained from this study may pave a novel scientific path leading to successful immunomodulatory therapy of IPF.

Multiple human studies of pulmonary fibrosis have shown the emergence of macrophage populations that are not present in normal lungs and may promote fibrosis. scRNAseq data revealed there was substantial heterogeneity of pulmonary macrophages in the populations found in patients with IPF, whereas macrophages from lung transplant donors were relatively homogeneous (34). Another study also demonstrated the heterogeneity of macrophages found in patients with IPF. Although CD71 (transferrin receptor) was almost uniformly expressed in alveolar macrophages from healthy individuals, a distinct population of CD71-negative macrophages was found in patients with IPF (35). In addition, the frequency of CD71-negative macrophages correlated with subsequent mortality in these patients, suggesting that this cell population may play a detrimental role (35). Interestingly, the CD71-negative macrophages expressed high levels of the monocyte marker CD14, suggesting that they may have differentiated from circulating monocytes (35). In addition to the above studies, recent human and mouse data suggest that monocytes are recruited from circulation into the lung in response to tissue injury and differentiate into tissue macrophages that contribute to IPF pathogenesis (reviewed in References 7, 31, and 36). These studies have demonstrated that the tissue-infiltrating monocytes/macrophages promote fibrosis through the production of growth factors such as TGF-β, chemokines, and other profibrotic mediators that lead to fibroblast activation, myofibroblast differentiation, and extracellular matrix remodeling. In contrast, the current study suggests that some tissue-infiltrating monocytes/macrophages may have a counterregulatory antifibrotic function, and the expression of VISTA may indicate such an antifibrotic capability of host immune responses. Given that the possibility of antifibrotic host immune responses and their potential for IPF treatment have rarely been explored, VISTA may present a chance to harness the homeostatic antifibrotic immunomodulatory capability of the host immune system as a novel therapeutic approach for IPF treatment.

The current study raises several intriguing questions that remain to be answered: *1*) how VISTA expression is further upregulated on the monocytes/macrophages after tissue injury; *2*) if other immune cell subsets expressing VISTA also contribute to post-bleomycin fibrotic lung injury; *3*) whether macrophages can be differentiated into M2 cells in the absence of VISTA; and *4*) the role of other macrophage subtypes in post-bleomycin fibrotic lung injury. In addition, the binding partner for VISTA in this context has not been fully elucidated, although PSGL-1 (P-selectin glycoprotein ligand-1), V-Set, and Immunoglobulin domain containing 3 (VSIG3) were proposed as potential binding partners (37, 38). In this regard, the complex nature of ontogeny, functional plasticity/heterogeneity, and cell-intrinsic and -extrinsic factors that determine the fates of monocytes/macrophages in tissues has been significantly unraveled recently (39, 40). By casting the light of these recent discoveries on how VISTA functions in limiting tissue fibrosis, we may gain further mechanistic insight that brings us closer to establishing immunomodulatory therapies targeting VISTA for the successful treatment of IPF. Regardless, this is the first study to demonstrate the proof of concept for a role of VISTA as an antifibrotic molecule and for a therapeutic benefit of VISTA agonists in IPF. ■

Author disclosures are available with the text of this article at www.atsjournals.org.

Acknowledgment: The authors thank Dr. Erica Herzog for a critical review of the manuscript and Ms. Susan Ardito for excellent administrative assistance.

References

1. Ley B, Collard HR, King TE Jr. Clinical course and prediction of survival in idiopathic pulmonary fibrosis. *Am J Respir Crit Care Med* 2011;183: 431–440.
2. Lederer DJ, Martinez FJ. Idiopathic pulmonary fibrosis. *N Engl J Med* 2018;378:1811–1823.
3. Richeldi L, du Bois RM, Raghu G, Azuma A, Brown KK, Costabel U, *et al.*; INPULSIS Trial Investigators. Efficacy and safety of nintedanib in idiopathic pulmonary fibrosis. *N Engl J Med* 2014;370:2071–2082.

4. King TE Jr, Bradford WZ, Castro-Bernardini S, Fagan EA, Glaspole I, Glassberg MK, *et al.*; ASCEND Study Group. A phase 3 trial of pirfenidone in patients with idiopathic pulmonary fibrosis. *N Engl J Med* 2014;370:2083–2092.
5. Mora AL, Rojas M, Pardo A, Selman M. Emerging therapies for idiopathic pulmonary fibrosis, a progressive age-related disease. *Nat Rev Drug Discov* 2017;16:755–772.
6. Cruwys S, Hein P, Humphries B, Black D. Drug discovery and development in idiopathic pulmonary fibrosis: challenges and opportunities. *Drug Discov Today* 2020;25:2277–2283.
7. Shenderov K, Collins SL, Powell JD, Horton MR. Immune dysregulation as a driver of idiopathic pulmonary fibrosis. *J Clin Invest* 2021;131:e143226.
8. Sato S, Fujimoto M, Hasegawa M, Komura K, Yanaba K, Hayakawa I, *et al.* Serum soluble CTLA-4 levels are increased in diffuse cutaneous systemic sclerosis. *Rheumatology (Oxford)* 2004;43:1261–1266.
9. Isshiki T, Akiba H, Nakayama M, Harada N, Okumura K, Homma S, *et al.* Cutting edge: anti-TIM-3 treatment exacerbates pulmonary inflammation and fibrosis in mice. *J Immunol* 2017;199:3733–3737.
10. Celada LJ, Kropski JA, Herazo-Maya JD, Luo W, Creecy A, Abad AT, *et al.* PD-1 up-regulation on $CD4^+$ T cells promotes pulmonary fibrosis through STAT3-mediated IL-17A and TGF-β1 production. *Sci Transl Med* 2018;10:eaar8356.
11. Ni K, Liu M, Zheng J, Wen L, Chen Q, Xiang Z, *et al.* PD-1/PD-L1 pathway mediates the alleviation of pulmonary fibrosis by human mesenchymal stem cells in humanized mice. *Am J Respir Cell Mol Biol* 2018;58:684–695.
12. Geng Y, Liu X, Liang J, Habiel DM, Kulur V, Coelho AL, *et al.* PD-L1 on invasive fibroblasts drives fibrosis in a humanized model of idiopathic pulmonary fibrosis. *JCI Insight* 2019;4:e125326.
13. Duitman J, van den Ende T, Spek CA. Immune checkpoints as promising targets for the treatment of idiopathic pulmonary fibrosis? *J Clin Med* 2019;8:1547.
14. Wang L, Rubinstein R, Lines JL, Wasiuk A, Ahonen C, Guo Y, *et al.* VISTA, a novel mouse Ig superfamily ligand that negatively regulates T cell responses. *J Exp Med* 2011;208:577–592.
15. Flies DB, Wang S, Xu H, Chen L. Cutting edge: a monoclonal antibody specific for the programmed death-1 homolog prevents graft-versus-host disease in mouse models. *J Immunol* 2011;187:1537–1541.
16. ElTanbouly MA, Zhao Y, Nowak E, Li J, Schaafsma E, Le Mercier I, *et al.* VISTA is a checkpoint regulator for naïve T cell quiescence and peripheral tolerance. *Science* 2020;367:eaay0524.
17. Han X, Vesely MD, Yang W, Sanmamed MF, Badri T, Alawa J, *et al.* PD-1H (VISTA)-mediated suppression of autoimmunity in systemic and cutaneous lupus erythematosus. *Sci Transl Med* 2019;11:eaax1159.
18. Liu H, Li X, Hu L, Zhu M, He B, Luo L, *et al.* A crucial role of the PD-1H coinhibitory receptor in suppressing experimental asthma. *Cell Mol Immunol* 2018;15:838–845.
19. Wang L, Le Mercier I, Putra J, Chen W, Liu J, Schenk AD, *et al.* Disruption of the immune-checkpoint VISTA gene imparts a proinflammatory phenotype with predisposition to the development of autoimmunity. *Proc Natl Acad Sci USA* 2014;111:14846–14851.
20. Adams TS, Schupp JC, Poli S, Ayaub EA, Neumark N, Ahangari F, *et al.* Single-cell RNA-seq reveals ectopic and aberrant lung-resident cell populations in idiopathic pulmonary fibrosis. *Sci Adv* 2020;6:eaba1983.
21. Flies DB, Han X, Higuchi T, Zheng L, Sun J, Ye JJ, *et al.* Coinhibitory receptor PD-1H preferentially suppresses $CD4^+$ T cell-mediated immunity. *J Clin Invest* 2014;124:1966–1975.
22. Kim SH, Lee JY, Yoon CM, Shin HJ, Lee SW, Rosas I, *et al.* Mitochondrial antiviral signaling protein is crucial for the development of pulmonary fibrosis. *Eur Respir J* 2021;57:2000652.
23. Neumark N, Cosme C Jr, Rose KA, Kaminski N. The idiopathic pulmonary fibrosis cell atlas. *Am J Physiol Lung Cell Mol Physiol* 2020; 319:L887–L893.
24. Travaglini KJ, Nabhan AN, Penland L, Sinha R, Gillich A, Sit RV, *et al.* A molecular cell atlas of the human lung from single-cell RNA sequencing. *Nature* 2020;587:619–625.
25. Rodero MP, Poupel L, Loyher PL, Hamon P, Licata F, Pessel C, *et al.* Immune surveillance of the lung by migrating tissue monocytes. *eLife* 2015;4:e07847.
26. Kang MJ, Choi JM, Kim BH, Lee CM, Cho WK, Choe G, *et al.* IL-18 induces emphysema and airway and vascular remodeling via IFN-γ, IL-17A, and IL-13. *Am J Respir Crit Care Med* 2012;185: 1205–1217.
27. Misharin AV, Morales-Nebreda L, Reyfman PA, Cuda CM, Walter JM, McQuattie-Pimentel AC, *et al.* Monocyte-derived alveolar macrophages drive lung fibrosis and persist in the lung over the life span. *J Exp Med* 2017;214:2387–2404.
28. Zhang F, Ayaub EA, Wang B, Puchulu-Campanella E, Li YH, Hettiarachchi SU, *et al.* Reprogramming of profibrotic macrophages for treatment of bleomycin-induced pulmonary fibrosis. *EMBO Mol Med* 2020;12:e12034.
29. King TE Jr, Pardo A, Selman M. Idiopathic pulmonary fibrosis. *Lancet* 2011;378:1949–1961.
30. Kolahian S, Fernandez IE, Eickelberg O, Hartl D. Immune mechanisms in pulmonary fibrosis. *Am J Respir Cell Mol Biol* 2016;55:309–322.
31. Byrne AJ, Maher TM, Lloyd CM. Pulmonary macrophages: a new therapeutic pathway in fibrosing lung disease? *Trends Mol Med* 2016; 22:303–316.
32. Yuan L, Tatineni J, Mahoney KM, Freeman GJ. VISTA: a mediator of quiescence and a promising target in cancer immunotherapy. *Trends Immunol* 2021;42:209–227.
33. ElTanbouly MA, Zhao Y, Schaafsma E, Burns CM, Mabaera R, Cheng C, *et al.* VISTA: a target to manage the innate cytokine storm. *Front Immunol* 2021;11:595950.
34. Reyfman PA, Walter JM, Joshi N, Anekalla KR, McQuattie-Pimentel AC, Chiu S, *et al.* Single-cell transcriptomic analysis of human lung provides insights into the pathobiology of pulmonary fibrosis. *Am J Respir Crit Care Med* 2019;199:1517–1536.
35. Allden SJ, Ogger PP, Ghai P, McErlean P, Hewitt R, Toshner R, *et al.* The transferrin receptor CD71 delineates functionally distinct airway macrophage subsets during idiopathic pulmonary fibrosis. *Am J Respir Crit Care Med* 2019;200:209–219.
36. Henderson NC, Rieder F, Wynn TA. Fibrosis: from mechanisms to medicines. *Nature* 2020;587:555–566.
37. Johnston RJ, Su LJ, Pinckney J, Critton D, Boyer E, Krishnakumar A, *et al.* VISTA is an acidic pH-selective ligand for PSGL-1. *Nature* 2019; 574:565–570.
38. Wang J, Wu G, Manick B, Hernandez V, Renelt M, Erickson C, *et al.* VSIG-3 as a ligand of VISTA inhibits human T-cell function. *Immunology* 2019;156:74–85.
39. Trzebanski S, Jung S. Plasticity of monocyte development and monocyte fates. *Immunol Lett* 2020;227:66–78.
40. Ginhoux F, Guilliams M. Tissue-resident macrophage ontogeny and homeostasis. *Immunity* 2016;44:439–449.